An application of dynamic positioning control using wave feed forward

J.A. Pinkster (TUD), A.B. Aalbers (MARIN) and R.F. Tap (MARIN)

Report 1302-P August 2001

Published in International Journal of Robust and Nonlinear Control, Number 11, pp. 1207 - 1237,

TU Delft

Delft University of Technology

Faculty of Mechanical Engineering and Marine Technology

Ship Hydromechanics Laboratory

INTERNATIONAL JOURNAL OF ROBUST AND NONLINEAR CONTROL
Int. J. Robust Nonlinear Control 2001; 11:1207–1237 (DOI: 10.1002/rnc.603)

An application of dynamic positioning control using wave feed forward

A. B. Aalbers[1,*,†], R. F. Tap[1] and J. A. Pinkster[2]

[1]*Maritime Research Institute Netherlands, 2, Haagsteeg, P.O. Box 28, 6700 AA Wageningen, The Netherlands*
[2]*Technical University Delft, Ontwerp Constructive en Produktie, Mekelweg 2, 2628 CD, Delft, The Netherlands*

SUMMARY

The paper presents the results of model tests for a large tanker in which wave drift force feed forward was applied in the dynamic positioning control system. The estimation method of the nonlinear (second order) wave drift forces from the measurement of relative water motions at the side of a ship hull is presented. The estimated wave drift forces are used in the DP control system, to enhance the filter process of the extended Kalman filter, and in the required thruster set-points. The EKF uses the nonlinear equations of low-frequency ship motions on the horizontal plane, which are also presented.

The results of the model tests show that the use of wave drift force feed forward significantly improves the positioning accuracy in sea states with 3.5 m significant wave height or higher. Copyright © 2001 John Wiley & Sons, Ltd.

KEY WORDS: dynamic positioning; feed forward; model test validation

1. INTRODUCTION

1.1. History

Conventional dynamic positioning (DP) control for ships that have to stay in position is based on feedback of position and heading error and vessel drift and yaw. In the early 1970s it was found that applying a real time estimate of the wind force in the DP control loop resulted in significant improvement of the DP performance. This method, called wind feed forward was very effective for smaller vessels and drill ships, having large superstructures, so that the wind load on the vessel is the major environmental disturbing force.

In the early 1980s the use of dynamically positioned tankers for export of oil from offshore production sites became an interesting alternative to the use of pipe lines and (bow hawser) moored export tankers. An example is shown in Figure 1.

These large vessels have a relatively small superstructure and are therefore more affected by second order wave (drift) forces than by wind. This initiated the search for methods to obtain

* Correspondence to: A. B. Aalbers, Maritime Research Institute Netherlands, 2, Haagsteeg, P.O. Box 28, 6700 AA Wageningen, The Netherlands.
† E-mail: a.b.aalbers@marin.nl

Published online 28 August 2001

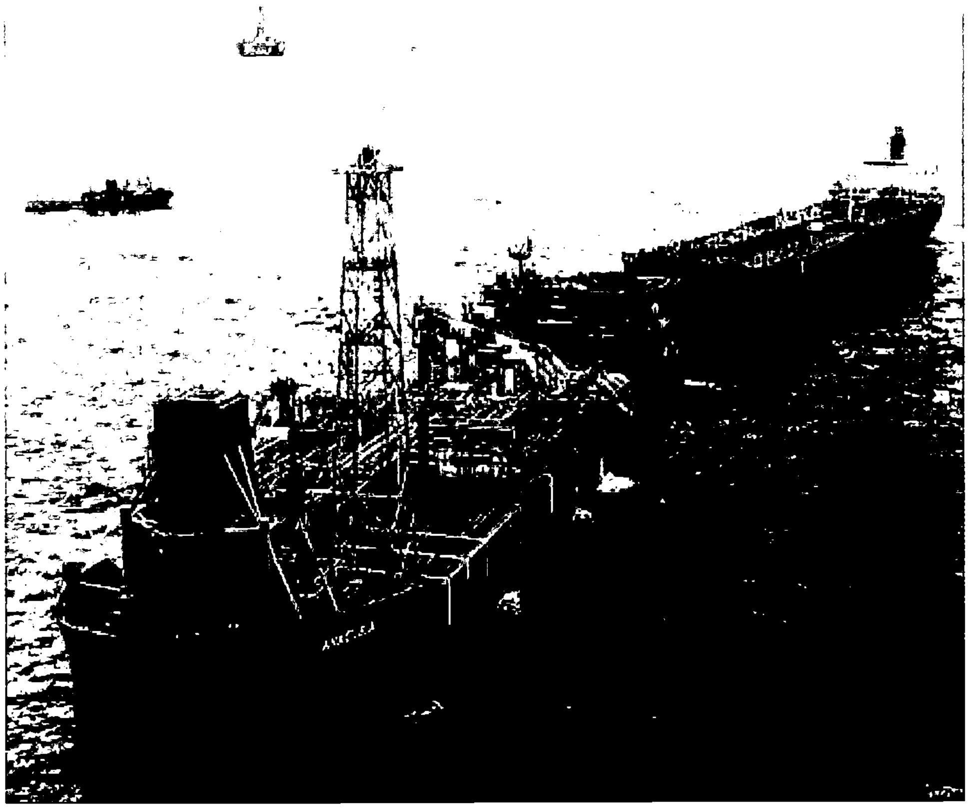

Figure 1. Picture of shuttle tanker behind FPSO.

a real time estimate of the wave drift force on the vessel, termed wave feed forward, to use in a similar way as the wind force estimate to improve the performance.

The underlying paper describes the methods used for real time estimation of wave drift forces and the application thereof in a DP control system used during closed-loop DP model tests at the Maritime Research Institute Netherlands. The vessel represented a large tanker ($L_{pp} \sim 240$ m), typical for a shuttle tanker or FPSO, but nowadays also comparable in size with the new generation drill ships. The model test research was supported by the contributions from industry and from the European Commission. The industry contributions were from BP Shipping, Gusto Engineering, Cégelèc projects (now Alstom Power Conversion), Harland & Wolff Shipbuilding and Bluewater Engineering.

The paper is structured as follows:

- Introduction with a summary of the theory of wave drift forces.
- Description of the real time estimation method for the wave drift forces acting on the model tested vessel.
- Description of the DP control system (incl. wave feed forward) used for the model tests.
- Description of the model test set-up, conditions and measurements.

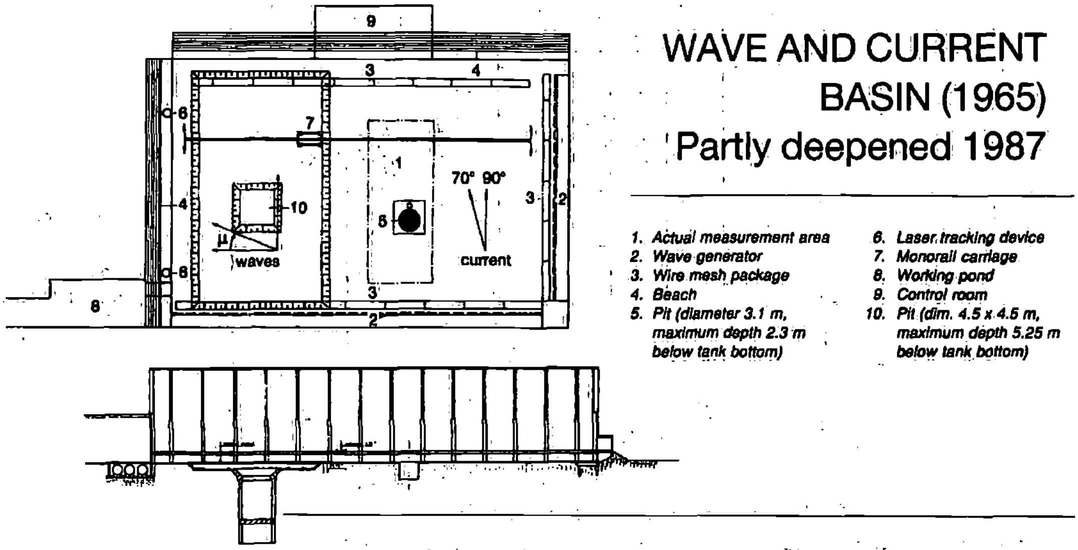

Figure 2.

- Results of the tests and discussion thereof, comparing DP positioning and power consumption in the same conditions with and without feed forward of the wave drift forces in the DP control.
- Conclusions.

The model tests were carried out in the Wave and Current basin of the Maritime Research Institute Netherlands, see Figure 2.

1.2. Wave drift forces

The waves at sea generate a slowly varying force on a floating object (e.g. a ship) so that it drifts, even in absence of current and wind. These forces originate from second-order processes in the interaction between the waves and the ship hull and have been described in detail by Pinkster [1].

The following gives a condensed description as far as relevant for the drift force estimation in the wave feed forward methodology. Use is made of potential theory with $\phi(\underline{x}, t)$ the local time dependent velocity potential in the fluid (see Reference [2]). The gradient of ϕ is the local fluid velocity and the time derivative ϕ_t, is proportional to the local pressure. See the Appendix.

The mathematical description of the wave drift force from pressure integration techniques is

$$\mathbf{F} = -\frac{1}{2}\int_{WL} \rho g s_r^2\, \underline{n}\cdot d\underline{l} + \underline{\alpha}^*(M\ddot{\underline{x}}_g) + \iint_S \frac{1}{2}\rho|\nabla\phi|^2\underline{n}\cdot d\underline{S} - \iint_S \rho(\underline{x}\cdot\nabla\phi_t\underline{n})\cdot d\underline{S} + \iint_S \rho\phi_t^{(2)}\underline{n}\cdot d\underline{S} \tag{1}$$

This expression is obtained by Taylor-series expansion of the pressures, motions and subsequent forces up to second order. The five contributions are:

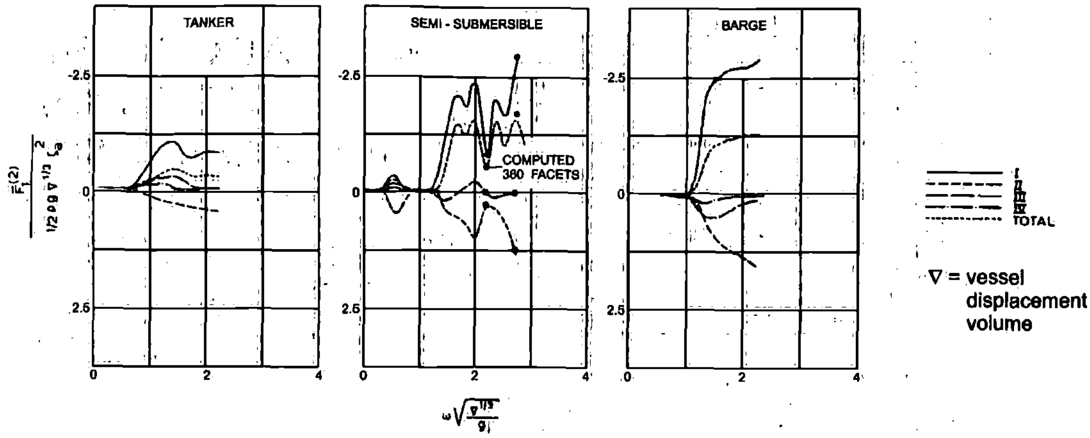

Figure 3.

1. The first contribution is the drift force contribution from the relative water motion around the hull, as will be elaborated below.
2. The second contribution is an interaction effect between the vessel's angular motions and its translational bodily accelerations.
3. The third contribution is from the hydrodynamic pressure in Bernoulli's Law.
4. The fourth is caused by interaction of local translations of the vessel hull in a pressure gradient.
5. The fifth contribution is due to the so-called 'set-down' waves, a strong effect in shallow water (water depth < 0.5 wave length).

The first term of Equation (1) is the most important contribution. The term stems from the fact that the pressure near the varying wetted surface due to the motions and diffraction will also give rise to a second-order contribution.

Basic physics learns that the total force on the vessel is the sum of all pressures acting on the wetted hull: $\mathrm{F} = -\iint_s p\underline{n}\cdot \mathrm{d}\underline{S}$. Now, let us look at the contribution near the waterline of the vessel, where the pressures vary due to waves.

The pressure in the waterline is the time derivative of the velocity potential ϕ of the wave

$$-\rho\phi_t = \rho g\zeta \tag{2}$$

which, when inserted will produce

$$\mathrm{F}_i = -\int_{\mathrm{WL}}\int_{z_{\mathrm{WL}}}^{\zeta}[-\rho g z + \rho g\zeta]\,\underline{n}\,\mathrm{d}z\cdot \mathrm{d}\underline{l} \tag{3}$$

The relative wave height is defined by

$$s_r = \zeta - z_{\mathrm{WL}} \tag{4}$$

Substitution of (4) into (3) and evaluation of the integration over z results in the first term of Equation (1). The term implies that the wave drift force is proportional with the (waterline integral of the) relative motion squared.

In Figure 3 the relative importance of the various contributions is illustrated, according to computations carried out by Pinkster [1] for regular waves in which the fifth contribution is zero.

1.3. *The effect of wave drift forces*

Wave drift forces may not be very large in magnitude, but they have a non-zero mean and are relatively slowly varying as shown in Figure 4. However, with a high wave group passing, the magnitude may rise quickly to levels which may be an order of magnitude larger than the mean level. This is caused by the fact that the wave drift forces are proportional to the square of the wave height. In Section 1.5 the statistical properties of drift forces are discussed.

The effect on a dynamically positioned vessel may be quite significant. The passage of a high wave group may push a ship from its heading, exposing more of its side to the incoming waves. The wave drift forces acting on it rise further and the vessel starts to drift 'bodily' from its position. A feedback controller will start to generate restoring forces on position error and drift velocity, but initially these are much smaller than the drift forces acting on the vessel with its side largely exposed. So, large position error may be the result. Such events occur all too often when the ship is positioning in a sea state close to its capability limits. In Figure 5 the position plot of such an event during model testing is shown, in which the vessel only just escaped from a complete drift off.

1.4. *Computation of the wave drift forces for an irregular sea spectrum*

Assume a known wave spectrum $S_\zeta(\omega)$. The mean drift force in that spectrum can be readily derived from

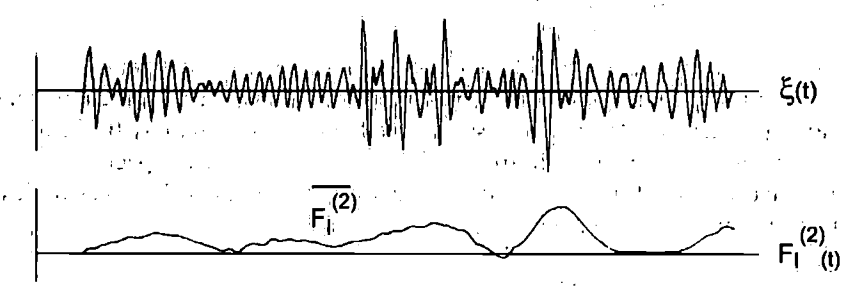

Figure 4.

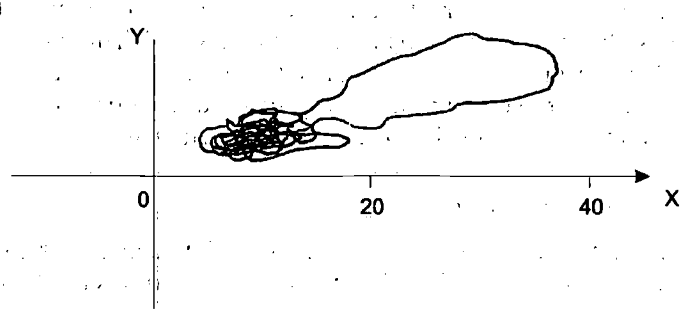

Figure 5.

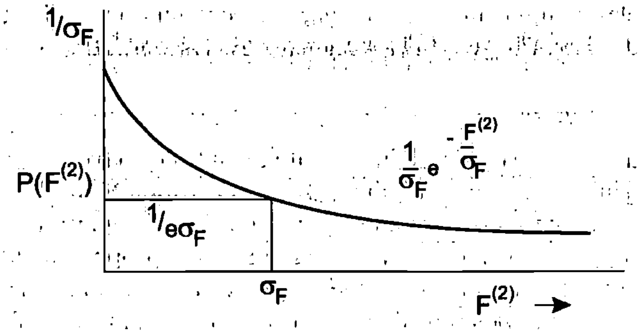

Figure 6.

$$F = 2\int_0^\infty T(\omega,\omega) S_\zeta(\omega)\,\mathrm{d}\omega \tag{5}$$

Herein $T(\omega,\omega)$ physically represents the mean wave drift force in a regular wave with frequency ω. The magnitude of the wave drift force quadratic transfer function $T(\omega,\omega+\mu)$ can be determined from sink-source potential theory computations using formula (1) in discretized frequency domain. The difference frequency of two regular waves, $\omega_i - \omega_j$ is represented as μ in the continuous formulations. The spectrum of the drift force is found from

$$S_F(\mu) = 8\int_0^\infty |T(\omega,\omega+\mu)|^2 S_\zeta(\omega) S_\zeta(\omega+\mu)\,\mathrm{d}\omega \tag{6}$$

Since the resolution with respect to the difference frequency μ must be large enough, this imposes the requirement that many frequencies have to be calculated. For example, if the natural period of the system is long (say about 150 s), a step size is needed of approximately 0.02 rad/s from the lowest up to the highest frequency with appreciable energy in the wave spectrum.

For the real time estimate of the wave drift force acting on the vessel the spectral descriptions derived in (5) and (6) are used, see Section 2.

1.5. Statistical properties of wave drift forces in a given sea spectrum

Based on the generally accepted assumption that wave elevation in a seaway follows a Gaussian distribution, and that the crest and trough heights follow a Rayleigh distribution, it was indicated by Pinkster [1] that the drift forces approximately follow an exponential distribution with a standard deviation equal to the mean. In Figure 6 such a distribution is shown and one can see that the maximum forces can be much higher than the mean value.

1.6. Wave drift forces in time domain

The wave drift forces are generated by second-order wave interaction with the vessel hull. If one would assume that $T(\omega,\omega+\mu) = 1$ for all values of μ, then expression (6) would reduce to

$$S(\mu) = 8\int S_\xi(\omega) S_\xi(\omega+\mu)\,\mathrm{d}\omega \tag{7}$$

TANKER HULL — **TOTAL**

ω_2 \ ω_1	0.354	0.444	0.523	0.600	0.713	0.803	0.887
0.354	2	9	10	25	10	38	37
0.444		7	21	19	26	12	35
0.523			12	16	8	14	14
0.600				14	10	18	15
0.713					9	4	7
0.803						9	5
0.887							9

T_{12} in tf/m²
Frequencies in rad./sec.

CONTRIBUTION I

ω_2 \ ω_1	0.354	0.444	0.523	0.600	0.713	0.803	0.887
0.354	10	19	27	23	21	20	21
0.444		25	32	31	26	28	28
0.523			32	34	27	30	27
0.600				31	29	29	27
0.713					23	27	25
0.803						25	28
0.887							25

T_{12} in tf/m²
Frequencies in rad./sec.

Figure 7.

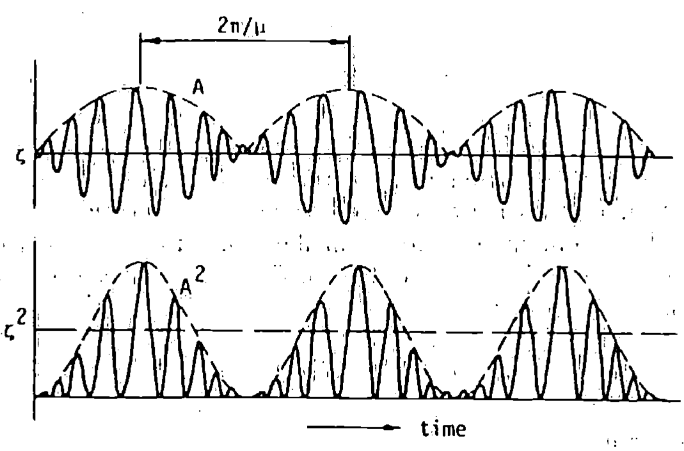

Figure 8.

This is the wave group spectral density, as can be derived from a 'sum of random phase sine waves' description of a sea. The wave drift force quadratic transfer function $T(\omega, \omega + \mu)$ is a complex function, of which the real part represents the force component which is in phase with the wave groups and the imaginary part represents the drift force components which are out of phase with the wave groups.

In the following section the estimating methods for the wave drift forces in time domain are described. In these methods use is made of assumptions with respect to the character of the wave drift forces.

The first assumption, used for method 1, is that the wave drift forces are well approximated by the first contribution times a correction factor. In Figure 7, tables are given of the first contribution and the total according to computations for a tanker by Pinkster [1]. The transfer function from contribution 1 is about twice the total. Also in other computations for monohulls such results are found.

The second assumption is used for the method 2, and comprises that the wave drift forces are to a large extent in phase with the wave groups. This can be acceptable if the length of a wave group is long with respect to the ship. A typical, large vessel for which wave feed forward is considered, measures about 250 m. A typical wave group consists of about 4 waves with a total length of

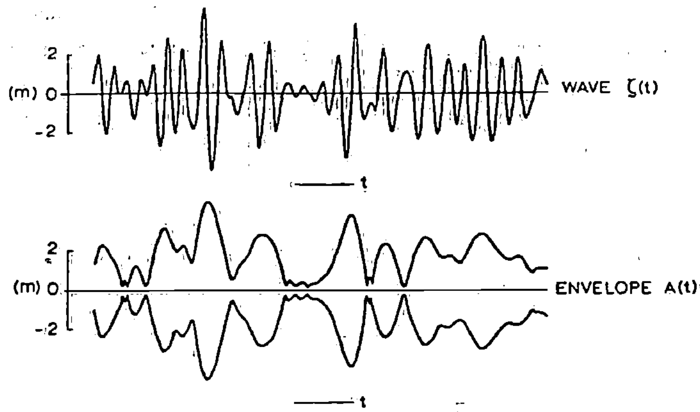

Figure 9.

about $4(g/2\pi)T^2$, in which T is the average wave period of the individual waves in the group. For a Beaufort 7 sea state in open sea, the wave period is about 8 s, so a typical group length is 350 m. This indicates that the assumption may be reasonably valid in the sea states of interest.

The wave groups are described in time domain from the sum of sine waves approach of describing a sea state:

$$\zeta(t) = \sum_{1}^{N} \zeta_i \cos(\omega_i t + \varepsilon_i) \tag{8}$$

which may also be written as

$$\zeta(t) = A(t)\cos(\omega_0 t + \varepsilon(t)) \tag{9}$$

The wave energy is defined by the Hilbert product of the wave height,

$$|A|^2(t) = \tfrac{1}{2}\zeta(t)\zeta(t)^* \tag{10}$$

Using Equation (8), and taking the low-frequency part only, the wave groups are defined by the low-frequency filtered part of the envelope squared:

$$A_{\mathrm{LF}}^2(t) = \sum_{1}^{N}\sum_{1}^{N} \frac{1}{2}\zeta_i\zeta_j \cos\{(\omega_i - \omega_j)t + (\varepsilon_i - \varepsilon_j)\} \tag{11}$$

For the sum of two sine waves the result is shown in Figure 8. For the wave group envelope of an irregular sea an example is given in Figure 9.

2. WAVE FEED FORWARD: WAVE DRIFT FORCE ESTIMATOR

2.1. *Assumptions*

As follows from the previous section, the basic assumptions for the estimation process of the wave drift forces in real time, according to the two methods that will be described, are respectively:

Method 1: The wave drift forces are dominated by the relative motion contribution.
Method 2: The wave drift forces are in phase with the envelope of the wave groups.

In both methods the wave drift forces are quantified through analysis of the relative motions along the hull. The first mentioned method is described by Pinkster [3] and requires many measurement locations around the hull of the vessel. The second approach is derived from the notion that a good estimate of the wave drift forces can be made if the wave direction with respect to the vessel is known. The method requires only three measurement locations on the bow and shoulders of the vessel (assuming that the vessel heading under DP will be with the bow into the waves). The method to estimate the dominant wave direction is first described by Aalbers and Nienhuis [4].

2.2. *Method 1. Using full integration along the waterline (with 10 wave probes)*

The wave drift force is estimated by numerical integration of the low-pass filtered pressure from the relative motion squared along the waterline, conform the first term in Equation (1):

$$-\frac{1}{2}\rho g \oint_{\mathrm{WL}} [s_r(x)]^2 \underline{n}\, \mathrm{d}\underline{x} \approx \mathrm{F}^{(2)}(t,\alpha_r) C_f \tag{12}$$

in which C_f is a correction factor to tune the magnitude of the total drift forces to that of the first contribution in Equation (1).

2.3. *Method 2. Based on wave direction measurement and using drift force transfer functions*

Measurement probes for the relative water motion at the side of the ship are located at the bow and at the shoulder on Port and Starboard side. These locations are chosen because for a vessel under DP in waves, the bow is normally heading more or less into the waves. The sensor at the bow is used to measure the average period T_{zs} and the 'envelope squared' $A_s^2(t)$ of the relative motion at the bow. The two sensors at Port and Starboard shoulder are used to derive the wave direction $\alpha_r(t)$. All these values: T_{zs}, $A_s^2(t)$ and $\alpha_r(t)$ are the result of averaging or low-pass filtering to be applicable in the time scale of wave groups instead of individual waves.

Since these filtering or averaging processes are leading to a phase lag, the method applies the information on T_{zs}, $A_s^2(t)$ and $\alpha_r(t)$ as if it is valid for the 'undisturbed' wave passing at the vessel midship. The travel time of the waves from bow to midship is approximately equal to the phase lag of the selected filters.

The theoretical basis of method 2 is described below. It starts with the basic notion that with standard numerical tools the mean wave drift force acting on a vessel in a given wave spectrum (with unit wave height) can be calculated as a function of the average (zero upcrossing) wave period and the wave direction. Using the wave envelope squared as modulation function, according to the assumptions derived from the previous section, the wave drift force on the vessel can be evaluated. This process is almost real time. However, instead of the wave period and envelope, the relative motion period and envelope are measured, so it is necessary to re-write the spectral equation (Equation (5)) for mean wave drift force as a function of relative motions.

It starts with the re-formulation of Equation (5) by substituting the expression for the mean wave drift force transfer function $T(\omega,\omega) = [\overline{\mathsf{F}^{(2)}}(\omega)/\zeta_a^2]$. Hence, for a given T_z and α_r of the wave

$$\begin{aligned}
\overline{\mathsf{F}^{(2)}(T_z,\alpha_r)} &= 2\int \frac{\overline{\mathsf{F}^{(2)}}(\omega)}{\zeta_a^2} S_\zeta(\omega)\,d\omega \\
&= 2\int \frac{\overline{\mathsf{F}^{(2)}}(\omega)}{s_r^2} \left|\frac{s_r^2}{\zeta_a^2}\right| S_\zeta(\omega)\,d\omega \\
&= 2\int \frac{\overline{\mathsf{F}^{(2)}}(\omega)}{s_r^2} S_s(\omega)\,d\omega \\
&= 2m_{0s}\int \frac{\overline{\mathsf{F}^{(2)}}(\omega)}{s_r^2} S_s^*(\omega)\,d\omega
\end{aligned} \tag{13}$$

Herein was used that $S_s(\omega) = m_{0s}S_s(\omega)^*$, where $S_s(\omega)^*$ is a unit relative motion spectrum depending on T_z and α_r.

Now, the estimate of the drift force from the relative motions is based on the following technique: Assume there is for each wave direction α_r and zero-upcrossing period T_z a wave spectrum that generates an unit relative motion at the bow with average zero upcrossing period T_{zs}. Take for a given wave direction this spectrum to be $BS_\zeta(\omega, T_z)$ with B such that

$$\int_0^\infty B\frac{s_r^2}{\zeta_a^2} S_\zeta(\omega, T_z)\,d\omega = 1. \tag{14}$$

Hence, the unit spectra of the relative wave height at the bow are given by

$$S_s^*(\omega, T_{zs}) = B\frac{s_r^2}{\zeta_a^2} S_\zeta(\omega, T_z) \tag{15}$$

The values of B and T_{zs} can be tabulated as a function of T_z and α_r.

From Equation (13) follows that the average drift force caused by the unit relative bow motion spectrum is

$$\overline{\mathsf{F}}_*^{(2)}(T_{zs}) = 2\int_0^\infty \frac{\overline{\mathsf{F}}^{(2)}(\omega)}{s_r^2} S_s^*(\omega, T_{zs})\,d\omega \tag{16}$$

The value of $\overline{\mathsf{F}}_*^{(2)}$ can be tabulated as a function of T_{zs} and α_r and is a 'mean drift force level indicator'. Multiplying this indicator with the magnitude of the prevailing value of the relative motion spectrum, m_{0s}, yields the prevailing value of the average wave drift force

$$\overline{\mathsf{F}}^{(2)}(t) = m_{0s}\overline{\mathsf{F}}_*^{(2)}(T_{zs}, \alpha_r) \tag{17}$$

The m_{0s} of the relative wave height and its T_{zs} can be determined from averaging the measurements, with:

$$m_{0s} = \frac{1}{\Delta T}\int_{t-\Delta t}^{t} s_r^2\,dt \tag{18}$$

In Equation (18) the averaging period ΔT is a long period, typically 0.5 h, over which the sea condition is considered to be stationary in spectral and statistical sense.

The final stage of the computation is to make an estimate of the instantaneous wave drift force, using the measurement of the relative motion at the bow as follows:

$$\mathrm{F}_j^{(2)}(t) = \bar{\mathrm{F}}_j^{(2)}(t)\frac{s^2_{\mathrm{r,bow}}|_{\mathrm{LP}}}{\overline{s^2_{\mathrm{r,bow}}|_{\mathrm{LP}}}} \tag{19}$$

with $s^2_{\mathrm{r,bow}}|_{\mathrm{LP}} = 2A_s^2(t)$, the envelope squared, and $\overline{s^2_{\mathrm{r,bow}}|_{\mathrm{LP}}} = 2m_{0s(\mathrm{actual})}$. Due to the difference in time period for which $A_s^2(t)$ and $m_{0s(\mathrm{actual})}$ are evaluated, the quotient is the 'modulator' giving the real time variations of the drift force. The $m_{0s(\mathrm{actual})}$ may slightly differ from the m_{0s} of the theoretical spectrum used in Equation (18), since the actual wave spectrum normally deviates from the theoretical spectra. The long-term average (say 0.5 h) of the 'modulator' is close to 1.

The subscript $j = 1, 2$ stands for the components in x and y direction with respect to the ship. The moment component in the horizontal plane (ψ) cannot be directly determined in this approach of method 2 because of lack of information. For, the moment on the ship changes sign if a wave group passes midship. A simplified estimate is used, by using the computations to associate to each combination of T_{zs} and α_r a point of application of F_y with respect to the midships, x_{F_y}, and then use the estimate:

$$M_z(t) \cong x_{F_y} F_y \tag{20}$$

as wave drift moment acting on the vessel.

In this computation the wave direction is needed to solve Equation (17). The wave direction α_r follows from the relative motion measurements at the sides according to the method of Aalbers and Nienhuis [3], described in short below.

2.4. *Wave direction estimator*

The wave direction with respect to the vessel can be estimated from the difference in the relative motion at windward side and lee side. This estimation is based on the assumption that there exists in good approximation a wave-frequency independent ratio between the two. In the research framework for these DP model tests, computations and wave tests were carried out to demonstrate the accuracy of this assumption.

The computed relative motions are based on the pressure in the water line for the potential theory computations. In Figures 10 and 11 examples are given of computed relative motion response functions, together with the measured data from regular wave tests and irregular wave tests. From these results two conclusions can be drawn:

1. The computations and measurements agree quite well over a frequency interval of $0.3 < \omega < 1.1$ rad/s. This frequency interval is wide enough to cover the normal and limit operational sea conditions for DP vessels at sea.
2. The difference in relative motion response function at Port and Starboard side for e.g. a wave direction 30° off the bow is quite significant and consistent over the frequency range of interest.

For the vessel under consideration the measurement locations at the forward shoulders showed to give the most consistent and distinct difference between windward and lee side relative motions.

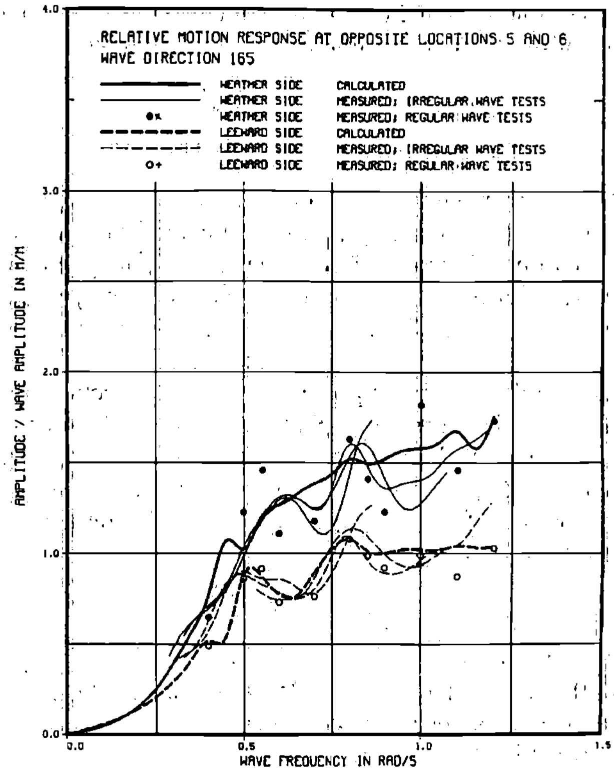

Figure 10.

The ration between the two is defined as

$$R(\alpha_r) = \int S_{s-\mathrm{PS}}(\omega)\,\mathrm{d}\omega \Big/ \int S_{s-\mathrm{SB}}(\omega)\,\mathrm{d}\omega \quad \text{for wave directions approaching from port (PS)}$$

and

$$R(\alpha_r) = \int S_{s-\mathrm{SB}}(\omega)\,\mathrm{d}\omega \Big/ \int S_{s-\mathrm{PS}}(\omega)\,\mathrm{d}\omega \quad \text{for wave directions approaching from startboard (SB)} \tag{21}$$

The graph in Figure 12 shows the ration as a function of wave direction for a range of wave spectra with average wave periods covering the operational sea states ($5 < T_z < 10$ s). The error margins in the graph indicate the standard deviation of the mean ration value for those spectra. This standard deviation is small so that a reasonable accuracy of the wave direction estimate may be expected.

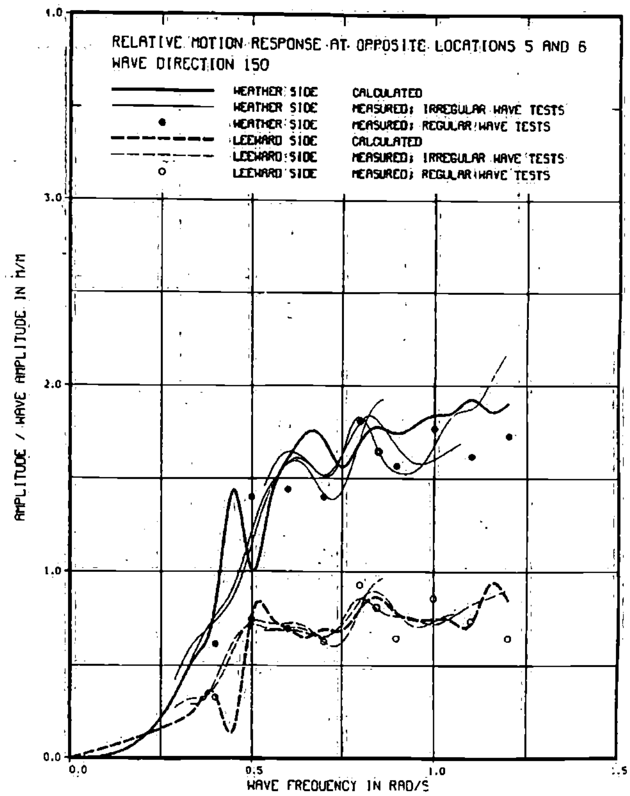

Figure 11.

2.5. Implementation

The relative wave height sensor positions on the model are shown in Figure 13, where all positions were used for method 1 and the numbers 1, 5 and 6 for method 2. (Note: the numbering corresponds to the positions defined for the numerical preparation work.) Defining $s_{r,i}$ as the relative wave height of sensor i and $s_{r,i}^2|_{LF}$ as the low-pass filtered squared relative wave heights, Equations (17), (19) and (21) were evaluated. The zero upcrossing period T_{zs} of the relative wave height at the bow is determined by counting the number of periods and computing the average period length over the time period ΔT that was also used in determining m_{0s} in Equation (18).

Causal type low-pass filters were used to obtain the low-frequency quantities (i.e. the envelope squared $A_s^2(t)$ of the relative motions at bow and shoulders) needed to evaluate the drift force modulation for Equation (19) and to derive the wave direction $\alpha_r(t)$ from Equation (21). The filter characteristics are shown in the Bode Diagrams of Figure 14. The selected filter has a -3 dB cut-off frequency of 0.016 Hz.

In Figure 15 the results are shown of the LP filtering of the relative motions measured in the model Test No. 23002, a condition with 6 m significant wave height approaching at an angle of 20° off the starboard bow.

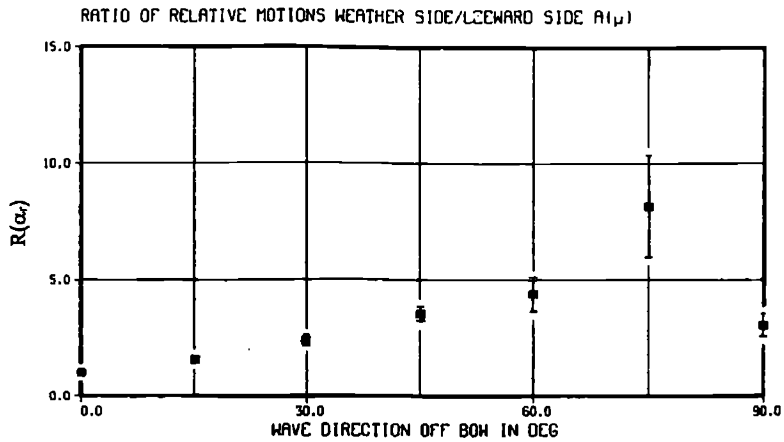

Figure 12.

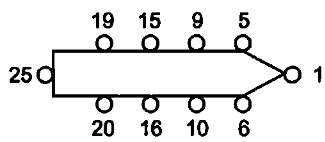

Figure 13.

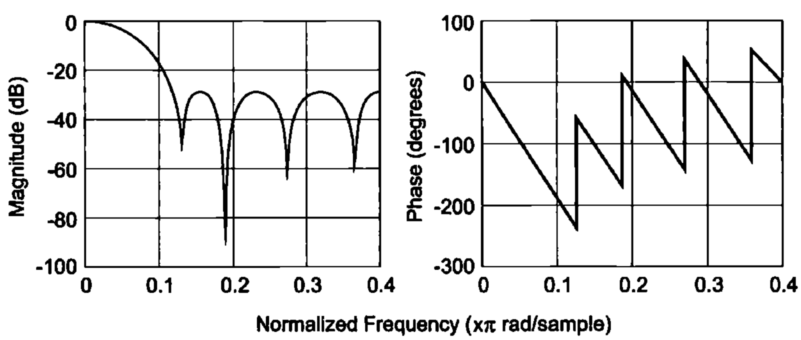

Figure 14.

3. DP CONTROL SYSTEM

3.1. DP model test configuration

The model tests were carried out using a tanker hull form at scale 1–50, equipped with a single, large size azimuthing thruster at the bow and at the stern. Each model thruster represented a combination of several thrusters in reality. More details of the physical modelling is given in

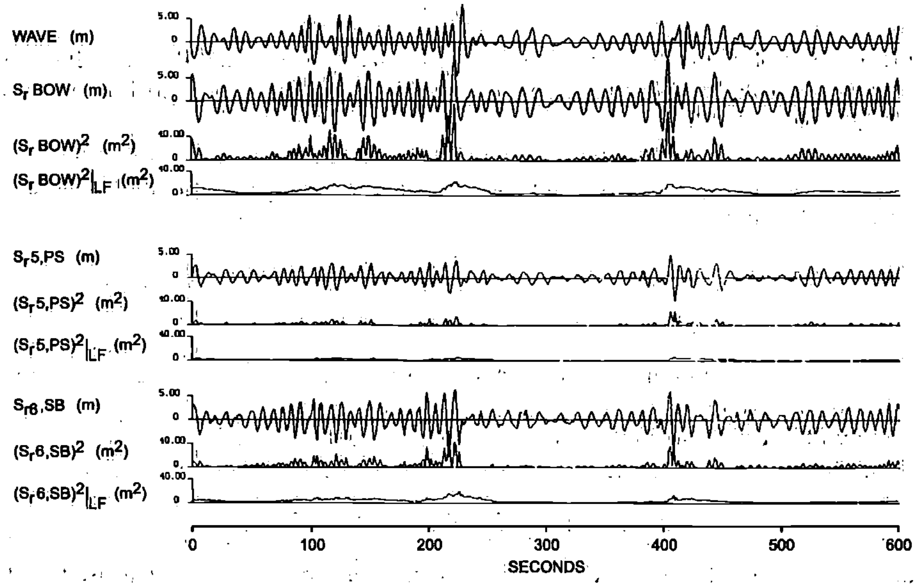

Figure 15.

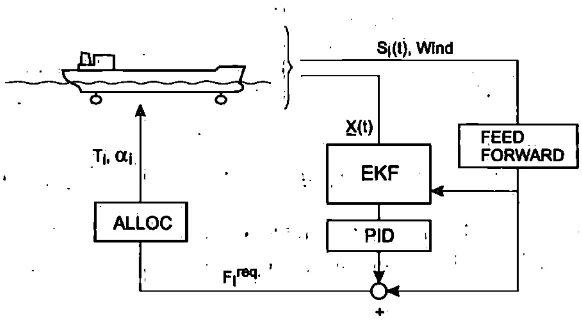

Figure 16.

Section 4. The dynamic positioning system in the basin (RUNSIM) uses a low-frequency Kalman filter for low-frequency position control. The control loop is shown in Figure 16 and has the following main components:

- Low-frequency extended Kalman Filter.
- Feed-back position control module on basis of PID coefficients.
- Optimum power thrust allocation.
- Wave drift force feed forward.

Although it would have been quite feasible with the available information from the feed forward module, there was no automatic heading optimisation implemented. The reason was that a straight comparison of DP performance on the same heading setpoint could be made between conventional and feed forward control.

3.2. The EKF

The condition for application of the extended Kalman filter (EKF) is that the underlying system is observable and controllable. For the present application of a dynamically positioned vessel these conditions are assumed valid.

The EKF is based on a nonlinear system- and measurement model in which $\underline{x}$ is the low-frequency vessel position, velocity and force vector in the horizontal plane. The description of the linearized and discrete system is

$$\underline{x}_{k+1} = A\underline{x}_k + B\underline{u}_k + G_k\underline{w}_k$$
$$\underline{y}_k = H\underline{x}_k + \underline{v}_k \tag{22}$$

where $\{w_k\}$ and $\{v_k\}$ are white noise, uncorrelated with x_0 and with each other. The matrix G_k is the projection of the system noise on $\underline{x}_{k+1}$.

The Kalman filter can be formulated in different ways, here is chosen for the recursive *a priori* formulation. The states are estimated recursively from the measurements according to Lewis [5]:

$$\hat{\underline{x}}_{k+1} = A\hat{\underline{x}}_{\bar{k}} + B\underline{u}_k + AK_k(\underline{y}_k - H\hat{\underline{x}}_{\bar{k}}) \tag{23}$$

Here $\hat{}$ denotes an estimate and $\bar{k}$ indicates that all information of $k = 1, \ldots, k$ is used. So the next state estimate equals the original model (22) corrected by a fraction of the prediction error, in which the Kalman gain K_k is defined by

$$K_k \equiv \hat{p}_{\bar{k}}H^{\mathrm{T}}(HP_{\bar{k}}H^{\mathrm{T}} + R)^{-1} \tag{24}$$

In Equations (24) and (25), the R and Q matrices are the covariance of the system and measurement noise w_k and v_k of the state equations in (22). The error covariance matrix $P_{\bar{k}}$ is also calculated recursively

$$P_{\bar{k}+1} = A[P_{\bar{k}} - P_{\bar{k}}H^{\mathrm{T}}(HP_{\bar{k}}H^{\mathrm{T}} + R)^{-1}HP_{\bar{k}}]A^{\mathrm{T}} + G_kQG_k^{\mathrm{T}} \tag{25}$$

Now the covariance matrix and state vector need only to be initialized. When P_0 has a large value, the filter converges fast. The value of $\underline{x}_0$ can be deduced from the first measurement.

3.3. The mathematical ship model

The vessel in question is a large tanker-type hull and the mathematical model in the EKF is described in detail by Nienhuis *et al.* [6]. The main aspects are reviewed below.

The *low-frequency* equations of motion are: (taking for ease of interpretation that x is surge, y is sway and ψ is yaw of the vessel in an earth-fixed, right handed co-ordinate system with the z-axis upward).

$$(M + a_{11})\ddot{x} = (M + a_{22})\dot{y}\dot{\psi} + F_x + F_{T_x}$$
$$(M + a_{22})\ddot{y} + a_{26}\ddot{\psi} = -(M + a_{11})\dot{x}\dot{\psi} + F_y + F_{T_y}$$
$$a_{62}\ddot{y} + (I_6 + a_{66})\ddot{\psi} = M_z + M_{T_z} \tag{26}$$

With the notion that $\underline{u}$ represents the thruster forces, this is a state equation in the form of

$$\dot{\underline{x}} = f_1(\underline{x}) + f_2(\underline{u}) \tag{27}$$

The state equation has to be written in discrete linearized form of Equation (22) with use of

$$A_{\mathrm{LF}} = M_{\mathrm{LF}}^{-1} \frac{\mathrm{d}f_1}{\mathrm{d}X} \tag{28}$$

and

$$A_{k,\mathrm{LF}} = I + A_{\mathrm{LF}} \Delta t \tag{29}$$

in which I is the unit vector.

3.4. *Feed forward control*

The external forces acting on a dynamically positioning vessel at sea are caused by

1. Current.
2. Waves.
3. Wind.
4. Thrusters.
5. Hydrodynamic reaction forces.

For some applications, e.g. DP-assisted moored FPSOs and pipe-laying vessels, additional external forces exist. These are not considered here but can be treated in a similar way.

By using real time estimates of the forces on the ship, the quality of the filter can be improved. In this way external forces can be taken into account before their effect is noticed in the form of position error and drift velocity. This is done in three steps. *Firstly*, the thruster forces and moment are taken into account by the term $f_2(u)$ in Equation (27). *Secondly*, knowing the LF displacement and velocities, the hydrodynamic reaction forces can be calculated on the assumption that the added mass and coupling terms in Equation (26) are constant. *Thirdly*, the environmental forces have to be estimated and used as a 'measurement'. When the ship stays on the same position the sum of all forces equals 0. So, the basic assumption is

$$\bar{\mathsf{F}}_{\mathrm{thr}} = -\{\bar{\mathsf{F}}_{\mathrm{win}} + \bar{\mathsf{F}}_{\mathrm{wav}} + \bar{\mathsf{F}}_{\mathrm{cur}} + \bar{\mathsf{F}}_{\mathrm{reac}}\} \tag{30}$$

In conventional DP control systems the current and wave forces ($\mathsf{F}_{\mathrm{cur}}$ and $\mathsf{F}_{\mathrm{wav}}$) are not known. The required thruster force ($\mathsf{F}_{\mathrm{thr}}$) is known from the allocation algorithm and the wind force ($\mathsf{F}_{\mathrm{win}}$) can be estimated from the measured wind speed and direction (wind feed forward). Therefore $\mathsf{F}_{\mathrm{cur}}$ and $\mathsf{F}_{\mathrm{wav}}$ are estimated jointly as the so-called 'rest force':

$$\bar{\mathsf{F}}_{\mathrm{wav}} + \bar{\mathsf{F}}_{\mathrm{cur}} = -\{\bar{\mathsf{F}}_{\mathrm{thr}} + \bar{\mathsf{F}}_{\mathrm{reac}} + \bar{\mathsf{F}}_{\mathrm{win}}\} \tag{31}$$

In wave drift force feed forward DP control, with the wave drift force estimate available according to Section 2, Equation (31) can be further elaborated. It is possible to take out the quite strongly varying external force $\mathsf{F}_{\mathrm{wav}}$. Hence, the remaining estimate for the very slowly varying current force is

$$\bar{\mathsf{F}}_{\mathrm{cur}} = -\{\bar{\mathsf{F}}_{\mathrm{wav}} + \bar{\mathsf{F}}_{\mathrm{thr}} + \bar{\mathsf{F}}_{\mathrm{reac}} + \bar{\mathsf{F}}_{\mathrm{win}}\} \tag{32}$$

The environmental force values are used in Equation (25) for F_x, F_y and M_z.

Furthermore, the wave drift force estimate is used directly in the PID feed back loop by adding the forces F_x, F_y and M_z to the required positioning forces from the PID controller. The force components due to wind are treated in the same way. The advantage thereof is that thruster action will try to immediately compensate the effects of the varying wave drift and wind force. This is expected to improve vessel position keeping. The PID feedback control equation is, with $j = 1 \ldots 3$ for F_x, F_y and M_z modes:

$$F_{\mathrm{req},j} = -P_j \Delta x_j - D_j \dot{x}_j - (1/\Delta T) \int_0^{\Delta T} I_j \Delta x_j \,\mathrm{d}t + k_1 \mathrm{F}_{\mathrm{win},j} + k_2 \mathrm{F}_{\mathrm{wav},j} \tag{33}$$

with k_1 and k_2 the fractions to which feed forward is applied.

3.5. Allocation

The two azimuthing thrusters are required to deliver the above derived forces from the PID controller as follows:

$$\begin{aligned} T_1 \cos\alpha_1 + T_2 \cos\alpha_2 &= F_{\mathrm{req}\,x} \\ T_1 \sin\alpha_1 + T_2 \sin\alpha_2 &= F_{\mathrm{req}\,y} \\ T_1 x_1 \cos\alpha_1 + T_2 x_2 \cos\alpha_2 &= M_{\mathrm{req}\,z} \end{aligned} \tag{34}$$

in which T, α and x are the thrust, azimuth angle and longitudinal position of the thrusters 1 and 2.

One additional equation is needed to solve the four unknowns, hence a power minimization requirement is applied on the following expression for the total power of the thrusters:

$$P = T_1^{2/3} + T_2^{2/3} \tag{35}$$

If none of the thrusters is overloaded ($T \ngeq T_{\max}$), the above allocation is solved with a Newton Raphson iteration method. In case of one or both thrusters being overloaded, the solution is straightforward.

4. MODEL TEST SET-UP

The set-up in the basin is shown in Figure 17, and the tanker body plan in Figure 18. The photograph of Figure 19 shows the azimuthing thruster arrangement. The measurements during the tests were:

- Six d.o.f. motions of the ship model.
- Nozzle thrust, unit thrust, RPM, torque and azimuth angle of each thruster.
- Relative water motions at 10 locations.

The x, y and z motion as well as the yaw angle are measured with respect to a basin fixed co-ordinate system, pitch and roll are measured with a vertical reference gyroscope in the model.

The wave conditions during the tests represent Pierson Moskowitz-type irregular sea spectra. The set-up allows to also test in cross-seas, utilizing wave generators at two sides of the basin to make a typical wind sea and a swell. In Table I the test conditions are reviewed and in Table II the vessel particulars are given.

The test duration corresponded to 1 h full scale, and the measurements were statistically analysed. Furthermore, time traces and position plots were made for presentation of the results.

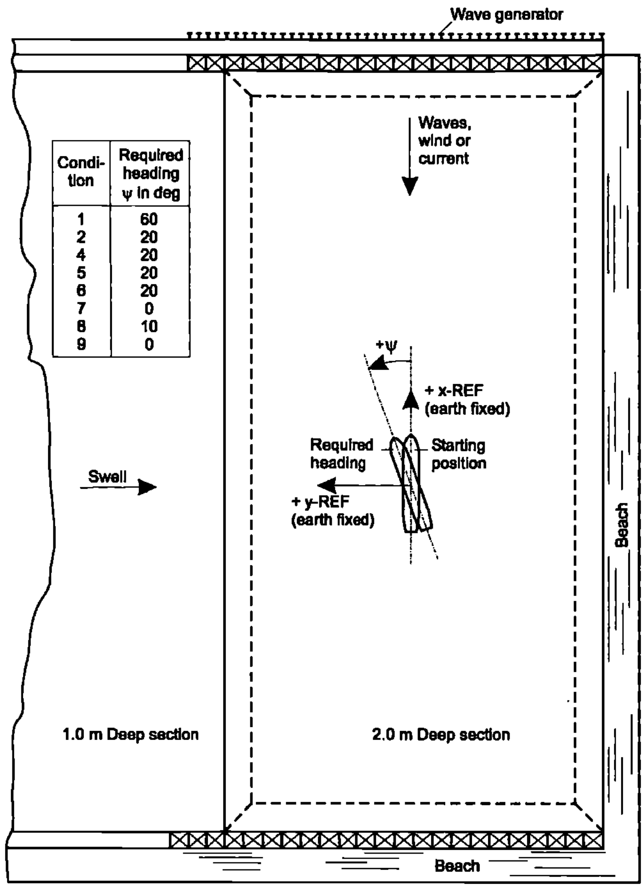

Figure 17.

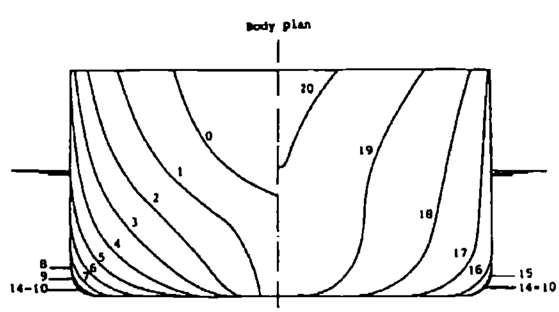

Figure 18.

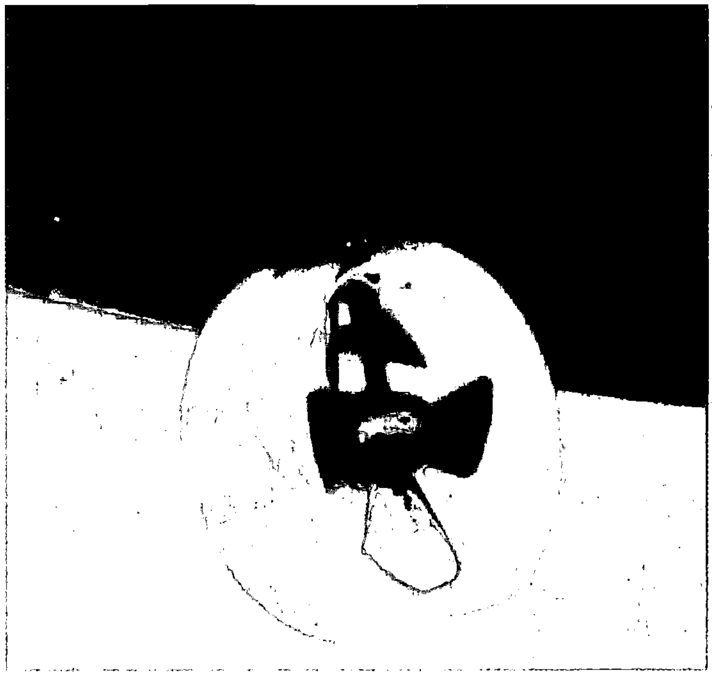

Figure 19.

Table I. Test review.

		Irregular sea				Swell			Wind		Current	
Required heading	Test condition	Dir. (deg)	H_S (m)	$T1$ (a)	Duration (min)	Dir. (deg)	H_S (m)	$T1$ (s)	Dir. (deg)	VW (kn)	Dir. (deg)	VC (kn)
60	1	180	2.0	6.0	30	—	—	—	180	15	180	1.0
20	2	180	2.0	6.0	60	—	—	—	180	15	180	1.0
20	3	180	2.0	6.0	60	—	—	—	180	15	90	1.0
20	4	180	3.5	7.0	60	—	—	—	180	30	180	1.0
20	5	180	3.5	7.0	60	270	2.0	8.0	180	30	—	
20	6	180	6.0	9.0	60	—	—	—	180	45	180	1.0
0	7	180	6.0	9.0	30	—	—	—	180	45	180	1.0
10	8	170	10.0	10.5	60	—	—	—	—	—	—	
0	9	180	10.0	10.5	60	—	—	—	—	—	—	

5. DISCUSSION OF THE RESULTS

5.1. Scope

The model tests with the DP tanker were carried out in a series of environmental conditions with wind, waves and current covering the normal and limit operational conditions. The heading

Table II. Main particulars and stability data of the tanker.

Designation	Unit	Magnitude
Length between perpendiculars	m	242.70
Breadth waterline	m	38.54
Depth	m	20.85
Draft fore	m	11.27
Draft mean	m	11.46
Draft aft	m	11.65
Displacement weight	TF	86 127
Centre of gravity above base	m	11.69
Centre of gravity forward of AP	mm	125.17
Transverse matacentric height	m	4.32
Longitudinal metacentric height	m	372.50
Transverse radius of gyration	m	12.22
Longitudinal radius of gyration	m	54.36
Vertical radius of gyration	m	54.36
Waterline area	m^2	8207.40

set-points for the DP control were selected on basis of normal practice: with the bow of the vessel more or less into the waves and wind. Note that the wave and wind directions are collinear except for the cross sea, where the swell direction is perpendicular to the wind. In most conditions, the current is parallel to the wind and waves, although one condition was tested with a cross current.

In this variety of test conditions, numbered 1–9 with increasing severity, test condition 1 is a short test with the heading set-point at 60°. Test conditions 8 and 9 were additional and represent an extreme storm sea, but without wind, in which the vessel was only just capable of keeping its position.

5.2. Results

In Figures 20 and 21 the time traces of a representative part of the tests in conditions 5 and 6 are shown, for conventional DP, for method 1 (with 10 relative motion probes) and method 2 (with three relative motion probes) respectively.

Condition 5 is a cross-sea condition (3.5 m wind sea and a 2 m swell) and the time traces show that:

- the position accuracy in X, Y and Ψ are better for the tests with Feed Forward;
- the thrust delivered by the two thrusters is about the same.

Condition 6 is a storm condition with 6 m seas. The time traces show that:

- the position accuracy in X, Y and Ψ are much better for the tests with Feed Forward;
- the thrust delivered by the two thrusters is slightly more (Method 2) or about the same.

In the next paragraphs the result of the test series will be discussed in more detail.

5.3. Summarized statistical results

Figures 22–24 show the mean and standard deviation values of the motions in the horizontal plane and of the delivered thrust. The mean value of the motions is not an indicator of the

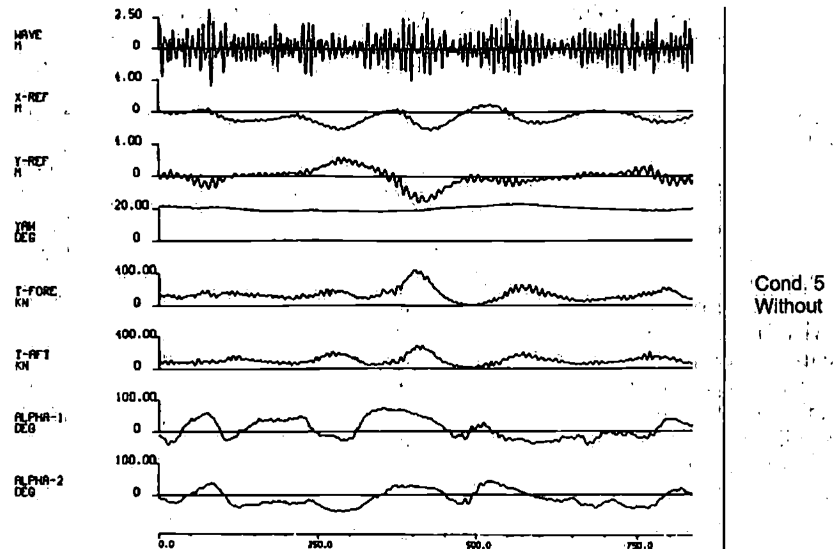
WAVE
M
X-REF
M
Y-REF
M
YAW
DEG
T-FORE
KN
T-AFT
KN
ALPHA-1
DEG
ALPHA-2
DEG
2.50
1.00
20.00
100.00
0
0.0
250.0
500.0
750.0
Cond. 5
Without

(a)

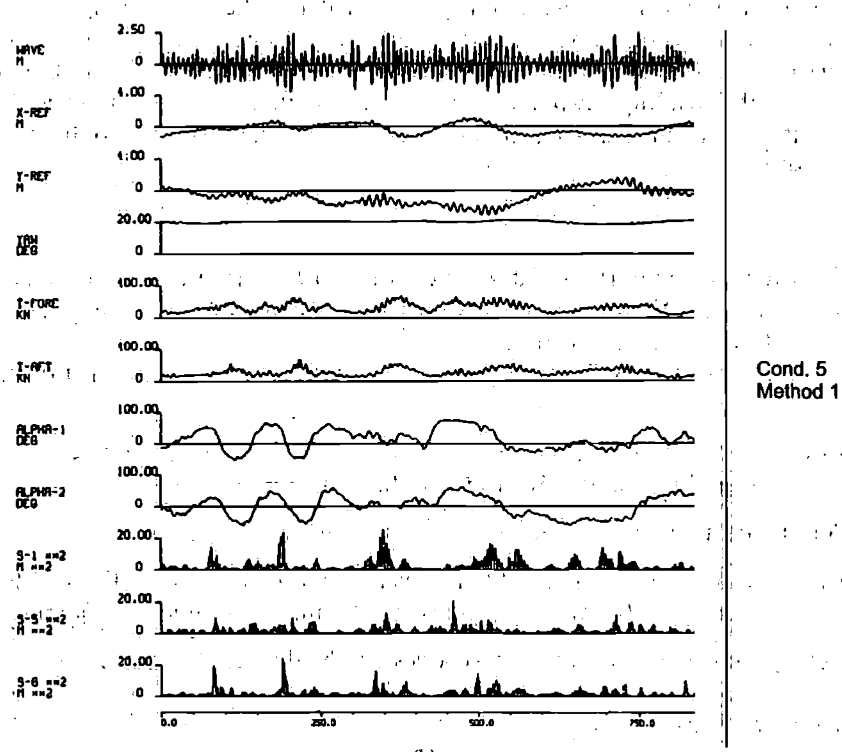
WAVE
M
X-REF
M
Y-REF
M
YAW
DEG
T-FORE
KN
T-AFT
KN
ALPHA-1
DEG
ALPHA-2
DEG
2.50
1.00
20.00
100.00
0
0.0
250.0
500.0
750.0
Cond. 5
Method 1

(b)

Figure 20.

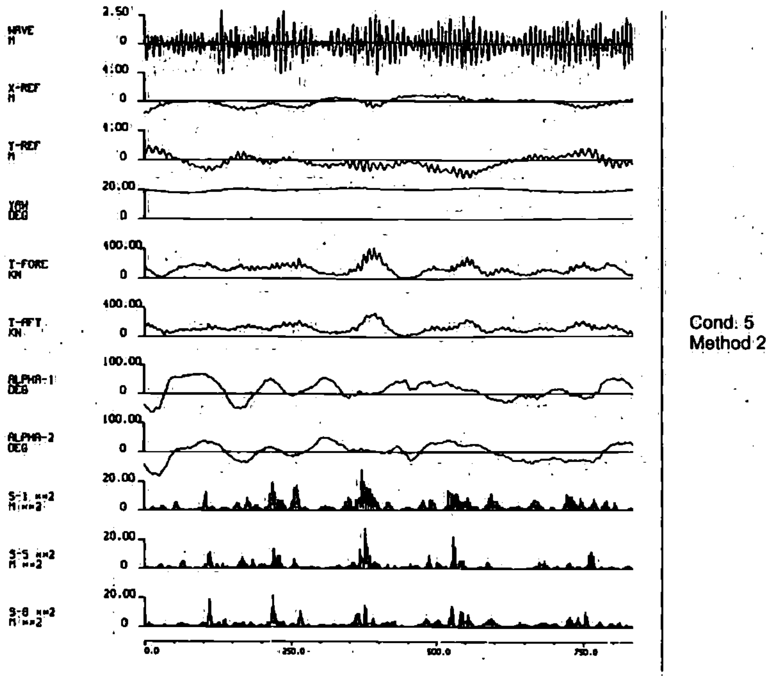

(c)

Figure 20. Continued.

positioning performance, because the DP system in the basin did not use the error integration of the PID controller, which would normally minimize the mean position error. So, for conventional control the mean position error is proportional with the mean environmental load (minus the wind force estimate, which is in feed forward) on the vessel. Reduction of the mean position error is found for the feed forward systems because the estimated wave drift force and wind force is immediately used in the required thrust.

The results will have to be considered with some care because for the tests with method 2 in conditions 1 and 4, the PID coefficients were 50 per cent lower than for the comparison tests.

5.4. Discussion

The results of the tests give as general conclusion that the use of wave feed forward improves the position standard deviations significantly for virtually the same thrust. The tests with method 2 in conditions 1 and 4 show deviating results because the PID coefficients were 50 per cent lower. This not only leads to larger position error, but also to significantly more delivered thrust. So, for these tests control was far less optimised than the other tests.

It can also be observed that method 1 gives slightly better positioning results than method 2, while for both methods the largest improvements were found in the X motion. This can be explained from a detailed analysis of the wave feed forward estimates as given below:

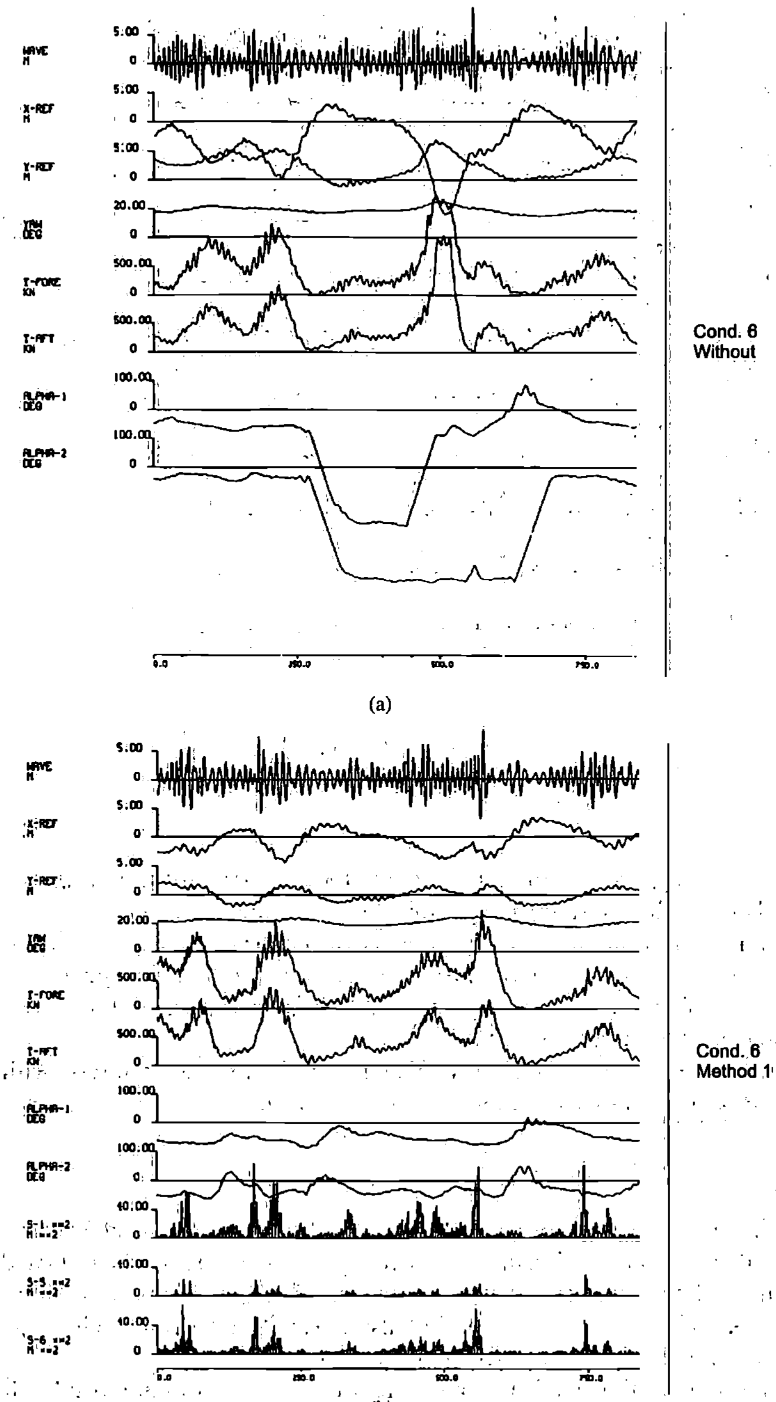

(a)

(b)

Figure 21.

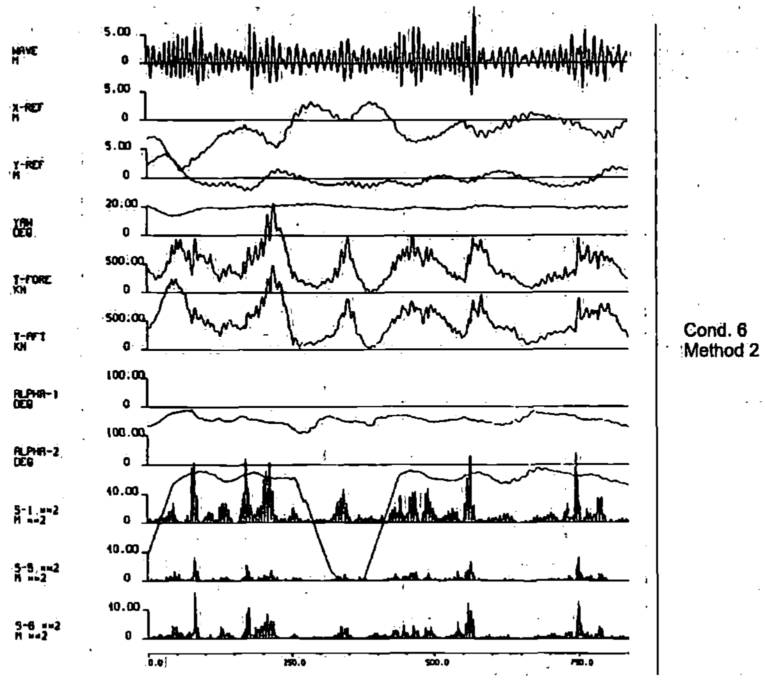

(c)

Figure 21. Continued

In Figure 25 the time trace of the estimated wave drift forces in X, Y and Ψ are given from methods 1 and 2 in condition 6. The values for X and Y in method 2 are higher than for method 1, while magnitude and character of the estimated drift moment from method 2 is quite different from that of method 1. The larger value of the X force estimate of method 2 may be the reason why in some of the tests an over-compensation of the mean position error is found, suggesting that the X force estimate is too high. A possible cause is that the numerical procedure assumed PM spectra, while the basin spectra deviated somewhat as shown in Figures 26 and 27 (3 and 6 m wave conditions). The same observation may apply to the Y force estimate. More important though is the difference in moment estimate. The simplification of Equation (19) ignores the fact that when a wave group passes the ship, the drift moment exerted on the vessel will change sign when the group passes the midship. The Y force keeps the same sign and so does the estimate for the moment from Equation (19).

Furthermore, it should be noted that the Y force estimate is quite dependent on the wave direction estimate from the relative motion sensors on the starboard and port side shoulder. In Table III the results are given of the wave direction estimates for several tests and compared with the actually measured values. The comparison shows that the direction estimate is surprisingly good. If for the cross sea an energy averaged wave direction is calculated, viz. 202.1°, the result is also good.

A shortcoming of the wave direction estimating method is that for wave directions more or less beam on to the vessel the function $R(\alpha)$ of Figure 12 may give an undefined solution. On the other

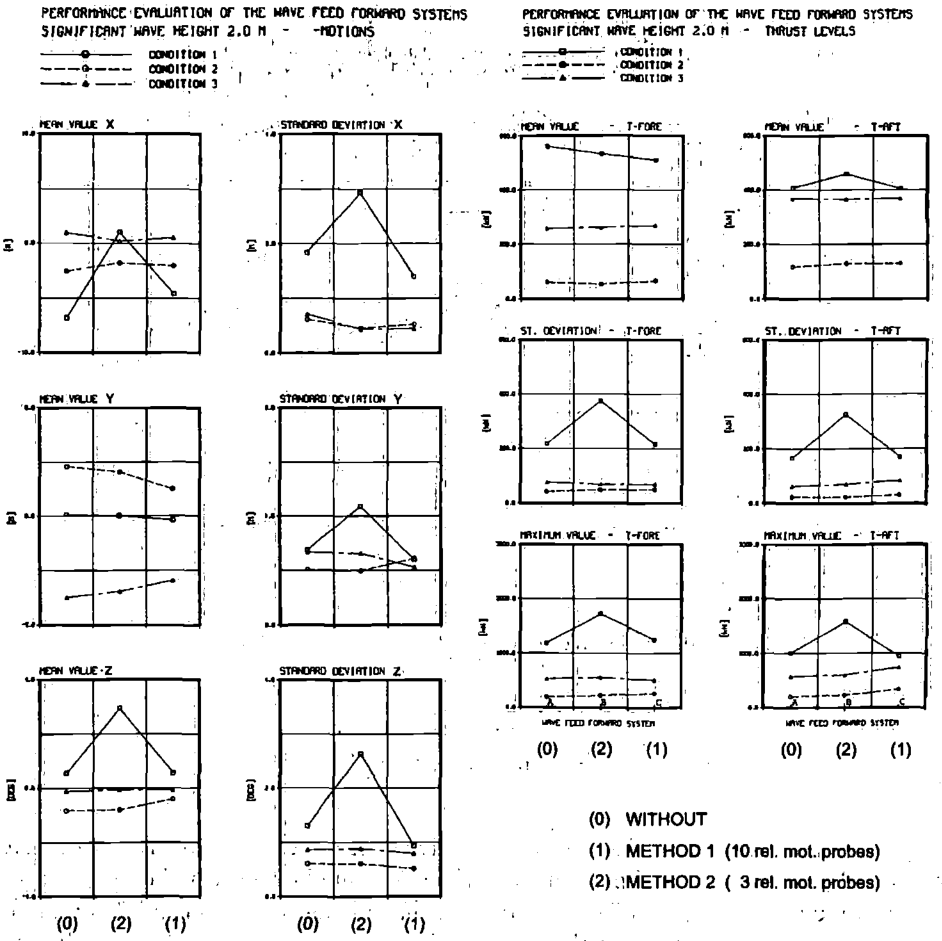

Figure 22.

hand it must be realised that the wave drift forces for wave directions around beam on are quite similar in magnitude. So, the error in wave direction does not necessarily lead to serious errors in the drift force estimates.

6. CONCLUSIONS

The DP control method with wave drift force feed forward was experimentally tested and a number of conclusions could be drawn:

- The real time wave drift force estimation methods 1 and 2 were somewhat different in quality, which was found back in the results, where the method 1, using 10 wave probes around the vessel, gave better results. The drift moment estimate of method 2 was too coarse, although the wave direction estimate was quite good.

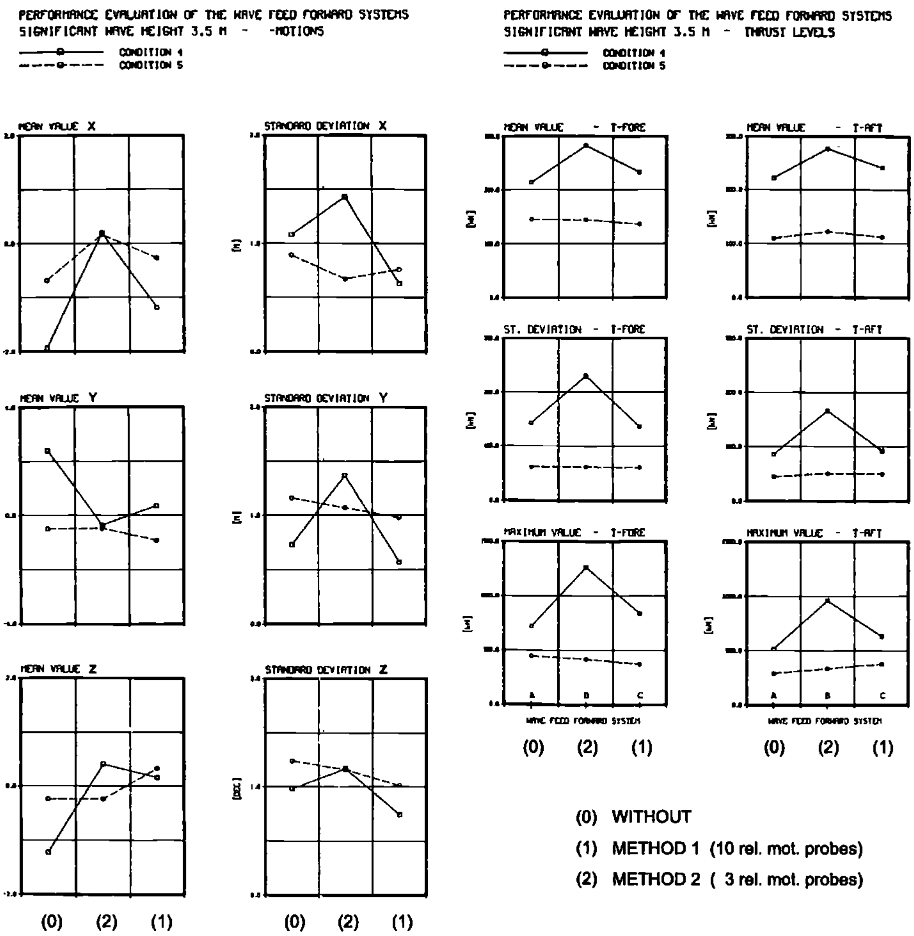

Figure 23.

- The application of wave drift force feed forward lead to improved positioning for the same power.
- The wave drift force estimates were calculated in a ‘plug on’ computation module, outputting the results to the EKF and to the required force for the thrusters. The advantage of this set-up is that it can be easily switched on and off.
- Further developments are needed to improve the wave drift force estimation and to allow method 2 to be used for all ship headings.

APPENDIX: NOMENCLATURE

ϕ = velocity potential
n = normal vector $\perp$ body surface

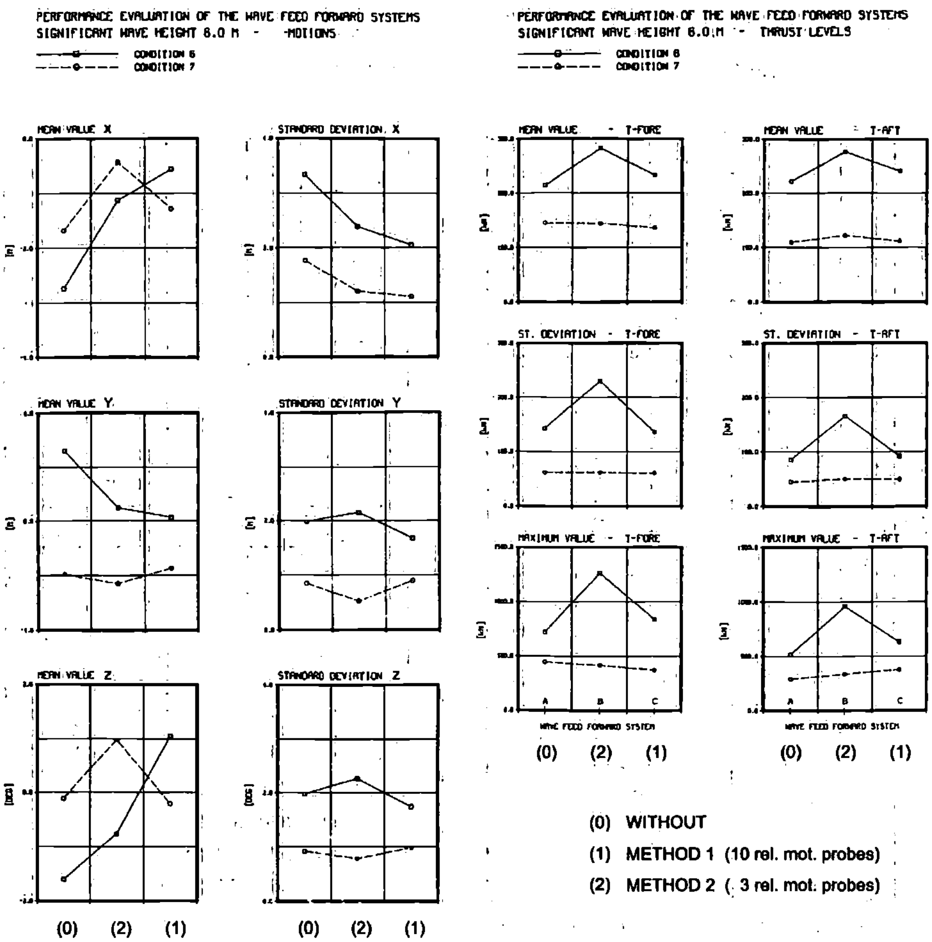

Figure 24.

z = depth co-ordinate
d = water depth
t = time
$_{,t}$ = time derivative
$\ddot{x}_G$ = translational acceleration in G
$\underline{x}$ = vector of local translations of a point on the ship hull
$\underline{\alpha}$ = vector of vessel angular motions
ω = frequency of oscillation
L = length of vessel
B = breadth of vessel
g = gravitational constant
ζ_a = wave amplitude
S = mean wetted area of vessel

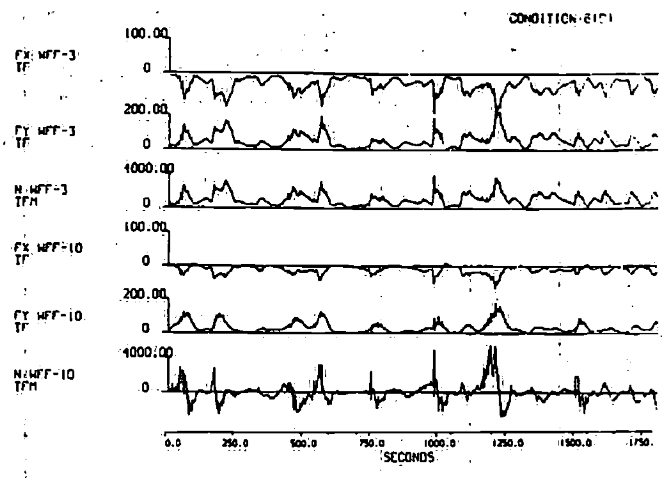

Figure 25.

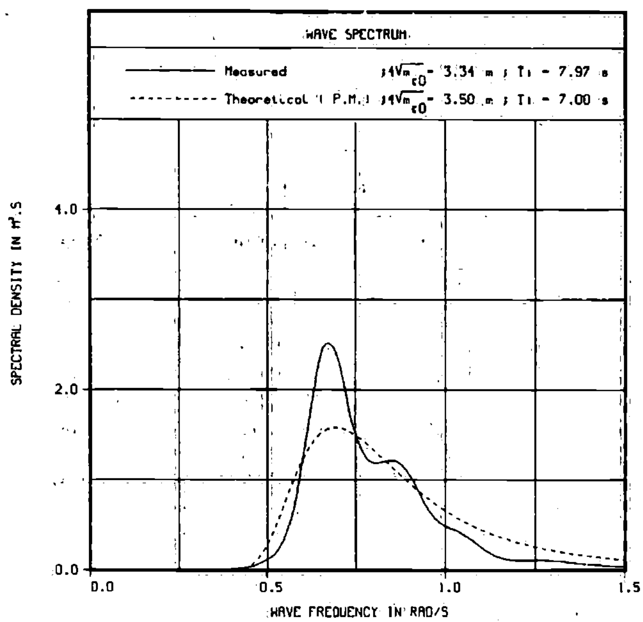

Figure 26.

$\mathbf{F}(\underline{\mathbf{x}}, \mathbf{t})$ = force vector
M = mass matrix of vessel
S_r = relative wave height at WL
$\bar{\mathrm{F}}_i$ = mean drift force in mode i
$\phi_i^{(2)}$ = second-order potential

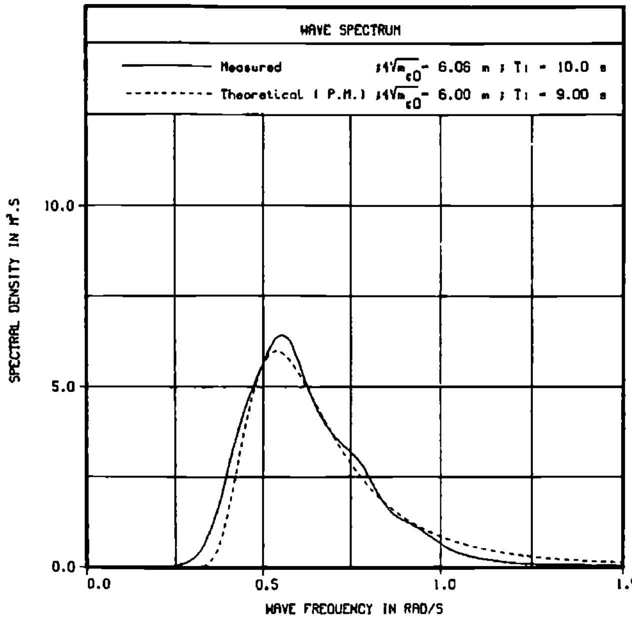

Figure 27.

Table III.

Test no.	Condition	Estimated wave direction		Measured wave direction	
		Mean	Standard dev.	Mean	Standard dev.
24501	1	188.4	0.30	180	1.31
23702	4	179.2	0.99	180	0.98
249301	5	197.6	0.88	Cross-sea	1.24
23201	6	185.6	0.52	180	1.98
25201	8	184.7	0.33	180	4.64
5501	9	183.6	0.18	180	2.14

$A^2(t)$ = envelope squared of wave
α_r = wave direction relative to ship
$B(T_z, \alpha_r)$ = correction coefficient
$S_F(\mu)$ = spectral density of wave drift force at μrad/s
$T(\omega_i, \omega_j)$ = quadratic transfer function
p = pressure
ρ = density of water
F_x, F_y, M_z = forces in x and y direction, and moment about z-axis respectively
z_{WL} = depth co-ordinate at waterline

State-space variables

$\underline{x}$ = state vector of position and velocity in the horizontal plane
$\underline{u}$ = thruster forces
$\underline{y}$ = observed vessel motions
T_i = thrust of thruster i
α_i = azimuth angle of thruster i
a_{ii} = added mass for mode of motion i
F_{T_x}, F_{T_y}, M_z = total thruster forces in x and y direction and total thrustler moment about z-axis respectively

REFERENCES

1. Pinkster JA. Low frequency second order wave exciting forces on floating structures. *Thesis*, Delft University of Technology, 1980.
2. Wehausen JV, Laitone EV. *Handbuch der Physik*, vol. 9. Springer: Berlin, 1960.
3. Pinkster JA. Wave-feed-forward as a means to improve dynamic positioning. *OTC* 3057, Houston, 1978.
4. Aalbers AB, Nienhuis U. Wave direction feed-forward on basis of relative motion measurements to improve dynamic positioning performance. *OTC* 5445, Houston, 1987.
5. Lewis FL. *Optimal Estimation*. Wiley, New York, 1986.
6. Nienhuis U, de Bock HJM, Braker PH. Simulations of DP vessels by model tests of computations. Maritime Research Institute Netherlands, September 1987.

